J Mol Model (2013) 19:2451–2458
DOI 10.1007/s00894-013-1796-x

ORIGINAL PAPER

Adsorption and decomposition mechanism of hexogen (RDX) on Al(111) surface by periodic DFT calculations

Cai-Chao Ye · Feng-Qi Zhao · Si-Yu Xu · Xue-Hai Ju

Received: 25 December 2012 / Accepted: 5 February 2013 / Published online: 24 February 2013

Abstract The adsorption of hexogen (RDX) molecule on the Al(111) surface was investigated by the generalized gradient approximation (GGA) of density functional theory (DFT). The calculations employ a supercell (4×4×3) slab model and three-dimensional periodic boundary conditions. The strong attractive forces between RDX molecule and aluminum atoms induce the N−O and N−N bond breaking of the RDX. Subsequently, the dissociated oxygen atoms, NO_2 group and radical fragment of RDX oxidize the Al surface. The largest adsorption energy is −835.7 kJ mol^{-1}. We also investigated the adsorption and decomposition mechanism of RDX molecule on the Al(111) surface. The activation energy for the dissociation steps of **V4** configuration is as large as 353.1 kJ mol^{-1}, while activation energies of other configurations are much smaller, in the range of 70.5–202.9 kJ mol^{-1}. The N−O is even easier than the N−NO_2 bond to decompose on the Al(111) surface.

Keywords Adsorption and dissociation · Al(111) surface · Density functional theory · Hexogen (RDX)

Introduction

Powderized aluminum (Al) is the most commonly used metallic additive in rocket propellant formulations to improve the performance of high energetic ingredients. Al powder is known to increase the combustion exothermicity and regression rate of solid propellant grains and enhance the blast effect of explosives as well as their underwater performance [1]. The efficiency of such processes depends on the size of the Al particles. Because of its large surface area, Al nanopowder can produce dramatic improvements in the performance of some energetic ingredients.

Hexogen (RDX), chemical name of hexahydro-1,3,5-trinitro-1,3,5-triazine ($C_3H_6N_6O_6$), is a well known high energetic density material (HEDM) [2, 3]. It has been widely used in solid propellant as an oxidizer. As Al nanopowder also is the most commonly used in solid propellants, it is important to understand the reaction in RDX/Al composite propellants. Up to now, researches have been carried out on the thermal behavior, decomposition mechanism, molecule structure, explosive performance and application of RDX [4–11]. Thermal decomposition of gas- and solid-phase RDX has been studied both experimentally and theoretically to understand the reaction pathways [4]. Boyd et al. carried out a molecular dynamics characterization of void defects in crystalline RDX to study the factors which affect the sensitivities of energetic materials to detonation initiation [5]. Umezawa et al. investigated the decomposition and chemisorption of RDX molecule on Al(111) surface using molecular dynamics simulations [6]. Balbuena employed DFT method to characterize the infrared and terahertz spectra of a RDX deposited over an aluminum surface, which was modeled as a planar cluster of Al_{16} [12]. Although there are extensive experimental and theoretical studies on the combustion of Al particle in air [13], only a few have reported its reaction characteristics with nitramine propellant such as RDX [6, 12, 14–19]. The content about its adsorption on Al surface is not comprehensive and decomposition mechanism for RDX on Al surface is not available. Our work focuses on the detailed atomic-level description of the interactions

Electronic supplementary material The online version of this article (doi:10.1007/s00894-013-1796-x) contains supplementary material, which is available to authorized users.

C.-C. Ye · X.-H. Ju (✉)
Key Laboratory of Soft Chemistry and Functional Materials of MOE, School of Chemical Engineering, Nanjing University of Science and Technology, Nanjing 210094, People's Republic of China
e-mail: xhju@mail.njust.edu.cn

F.-Q. Zhao · S.-Y. Xu
Science and Technology on Combustion and Explosion Laboratory, Xi'an Modern Chemistry Research Institute, Xi'an 710065, People's Republic of China

between the energetic compound of RDX and the Al(111) surface. The Al surface is considered to be easily exposed, easily oxidized and chemically corroded [20–22]. In this paper, we studied six adsorption configurations of RDX on Al(111) surface to see how the initial adsorption positions of RDX affect its decomposition pathways. In addition to studying the geometries and energies of adsorptions, we investigated the density of states as well. In view of the DFT calculations were employed to investigate the chemisorptions and dissociation pathways of NO on the Rh surfaces [23] as well as H_2S on the closed packed surfaces of a number of important noble metals and transition metals [24, 25], we also studied the decomposition mechanism of RDX molecule on the Al(111) surface with a periodic DFT approach.

Computational method

The calculations performed in this study were done using the CASTEP package [26] with Vanderbilt-type ultrasoft pseudopotentials [27] and a plane-wave expansion of the wave functions. Exchange and correlation were treated with the generalized gradient approximation (GGA), using the functional form of Perdew, Burke, and Ernzerhof of PBE [28]. The electronic wave functions were obtained by a density-mixing scheme [29] and the structures were relaxed using the Broyden, Fletcher, Goldfarb, and Shannon (BFGS) method [30]. In this study, the cutoff energy of plane waves was set to 300 eV. Brillouin zone sampling was performed using the Monkhost–Pack scheme. The values of the kinetic energy cutoff and the k-point grid were determined to ensure the convergence of total energies.

The Al surface was represented by a slab model with periodic boundary conditions. The energy convergence with respect to the number of layers has been tested to ensure the reliability and representative of the selected model. The surface energy (E_{surf}) is calculated by equation,

$$E_{surf} = \frac{E_{slab} - nE_{bulk}}{2A}, \quad (1)$$

here E_{slab} is total energy of the selected slab supercell, E_{bulk} is the energy of the bulk crystal per atom, n is the number of atoms in the slab calculation, and A is the area of the slab. The surface energies of 1, 2 and 3 layers are 0.40 eV, 0.35 eV and 0.35 eV, respectively. Therefore, considering the balance of both computational efficiency and accuracy, a 4×4 supercell with three layers containing 48 Al atoms was used to study the adsorption of the molecular systems (see Fig. 1). The slabs were separated by 16 Å of vacuum along the c-axis direction with a RDX molecule on the top of the slab. The cell size with a rhombic box of a×b×c is 11.45×11.45×18.34 Å.

Several tests have been performed to verify the accuracy of the method when applied to bulk aluminum and to the isolated RDX molecules, such as the optimum cutoff energy for calculations. For bulk aluminum, we have tested for convergence, using the k-point sampling density and the kinetic energy cutoff. In these calculations, a Monkhorst-Pack scheme with mesh parameters of 12×12×12 has been used, leading to 56k-points in the irreducible Brillouin zone. To determine the equilibrium bulk parameters of aluminum, we uniformly scaled the lattice vectors and performed energy calculations as a function of the unit-cell volume. The calculated lattice constants are the same values of 4.050 Å at E_{cut}= 300 eV and E_{cut}=400 eV. It can be concluded that, at E_{cut}=300 eV, the bulk structure is well converged, with respect to the cutoff energy. The calculated lattice constant of 4.050 Å is also identical to the experimental value [31], indicating that the present set of pseudo-potentials is able to provide a very good representation of the structural properties of bulk aluminum.

An equally good representation has been observed for the geometric parameters of the isolated RDX molecules. For example, on the basis of optimizations of the isolated RDX

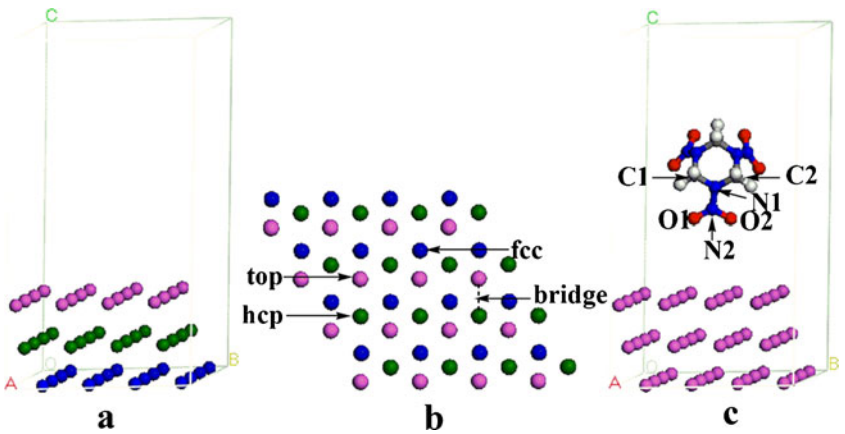

Fig. 1 **a** *Lateral view* of the slab model of Al(111). Atoms in different layers are colored differently for easy identification. **b** *Top view* of the surface. Surface sites are depicted in the panel. **c** RDX molecule on the Al surface with no interactions

molecule in a rhombic box with dimensions of 11.45×11.45×18.34 Å, we obtain the following equilibrium geometries of RDX molecule: r (N1−N2)=1.398 Å, r (N2−O1)=1.252 Å, r (N2−O2)=1.251 Å, r (C−N)=1.453–1.454 Å. Bond angles of θ (N2−N1−C)=121.0–121.1°, θ (N1−N2−O2)=116.5° and θ (N1−N2−O1)=116.6° at E_{cut}=300 eV. The increase of the cutoff energy to 400 eV leads to the following values: r (N1−N2)=1.404 Å, r (N2−O1)=1.250 Å, r (N2−O2)=1.251 Å, r (C−N)=1.454 Å, and θ (N2−N1−C)=120.3–120.7°, θ (N1−N2−O2)=116.7° and θ (N1−N2−O1)=116.3°. We noticed that there are no significant differences between the values obtained at the two cutoff energies, indicating the convergence of the results even at E_{cut}=300 eV. These values are also very close to the experimental data for crystal RDX (for example: N1−N2: 1.36 Å, N2−O1: 1.23 Å, N2−O2: 1.23 Å, and N2−N1−C: 118.7°) [8]. The good agreement between our calculated properties of aluminum bulk and the isolated RDX molecule with the experiment suggests that the performed computational method is proper to the adsorption system of RDX molecule on the Al(111) surface, which qualifies us for investigation of molecular adsorption on the Al(111) surface.

For the case of chemical adsorption configurations, the corresponding adsorption energy (E_{ads}) was calculated according to the expression

$$E_{ads} = E_{(adsorbate+slab)} - E_{(molecule+slab)}, \quad (2)$$

where $E_{(adsorbate\ +\ slab)}$ is the total energy of the adsorbate/-slab system after the RDX molecule being absorbed by Al slab and $E_{(molecule\ +\ slab)}$ is the single-point energy of the RDX/slab system as a whole but without interactions between RDX molecule and the Al slab (RDX molecule is as far as 6.1 Å away from Al surface).

The $E_{(adsorbate\ +\ slab)}$ and $E_{(molecule\ +\ slab)}$ were calculated with the same periodic boundary conditions and the same Brillouin-zone sampling. A negative E_{ads} value corresponds to a stable adsorbate/slab system. Figure 1 shows the Al slab model, the absorbed surface sites and the configuration of RDX molecule on the Al surface atoms with no interactions of adsorbate/Al.

Transition states (TS) were located by using the complete LST/QST method [32]. Firstly, the linear synchronous transit (LST) maximization was performed, followed by an energy minimization in directions conjugated to the reaction pathway. The TS approximation obtained in that way was used to perform quadratic synchronous transit (QST) maximization. From that point, another conjugate gradient minimization was performed. The cycle was repeated until a stationary point was located. The convergence criterion of the transition state calculations was set to 0.25 eV $Å^{-1}$ for the root-mean-square force. The activation energy is defined as: $E_a = E_{TS} - E_R$, where E_{TS} is the energy of transition state, and E_R is the sum of the energies of reactants.

Results and discussion

The adsorption and decomposition of RDX molecule on the Al(111) surface are complicated. There exist both physical and chemical adsorptions, and the latter case results in the

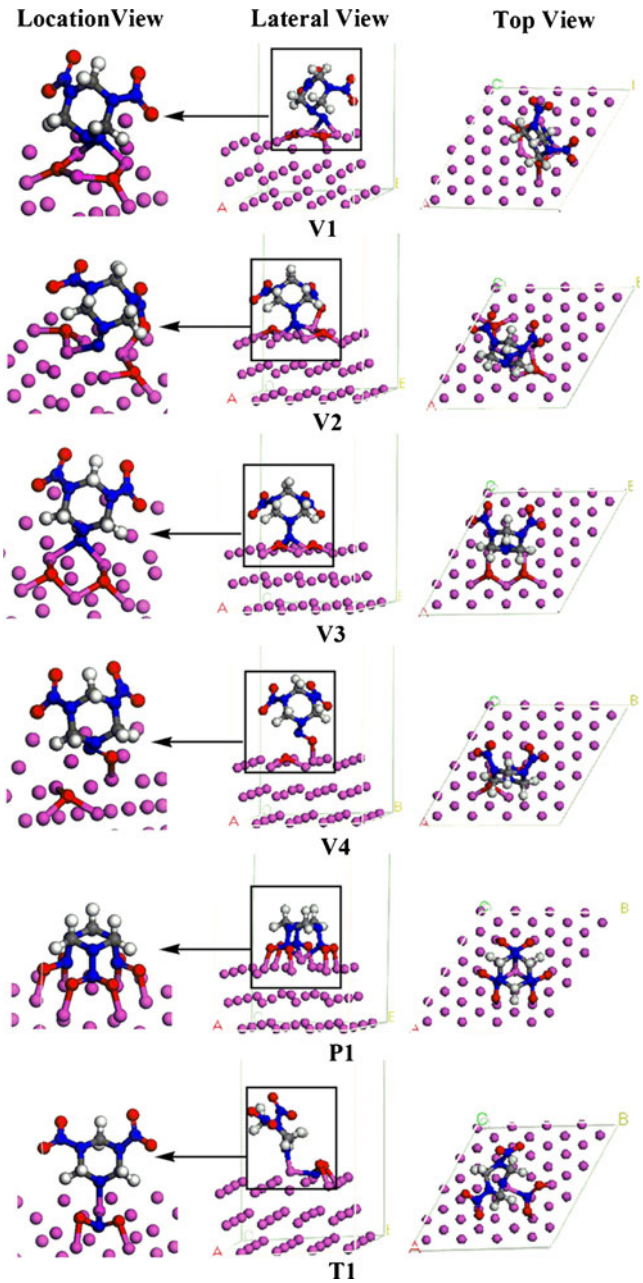

Fig. 2 Adsorption configurations of RDX on the Al(111) surface. V, P and T denote vertical, parallel and tilted adsorptions of RDX, respectively

decomposition of the RDX molecule on the Al surface. There are four cases as follows:

(1) The RDX molecule is nondissociative, for example, see Fig. 2, **P1**.

(2) 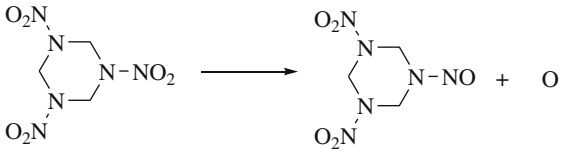

(3) 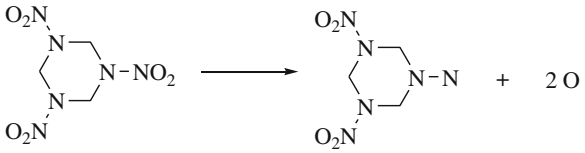

(4) 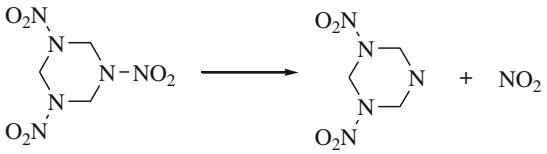

According to the orientation of the N1−N2 bond of RDX molecule relative to the Al(111) surface, **V1**, **V2**, **V3** and **V4** are four kinds of vertical adsorptions of RDX, they denote the N atom above a top site, an hcp site, a bridge site, and an fcc site, respectively, **P1** is one kind of parallel adsorption of RDX, as well as **T1** is a tilted adsorption of RDX. Moreover the lateral and top views of the optimized adsorption configurations after full relaxation of the atomic positions have been given in Fig. 2.

Geometries and energies

The adsorption energies were calculated by Eq. 2 and given in Table 1. As Fig. 2 shows, **V1** to **V4** show the adsorption configurations that the N1−N2 bond is initially vertical to the Al surface and above an on-top site, an hcp site, a bridge site, and an fcc site, respectively. **P1** is the adsorption configuration that RDX molecule was initially parallel to the Al surface, and **T1** is an adsorption configuration that RDX molecule was initially tilted to the Al surface. Adsorption at **V1** site leads to a complete dissociation of both O atoms of N2 nitro group. The N2 and two dissociated O atoms adsorb on Al surface, resulting in a total of two Al−N bonds and six Al−O bonds. The Al−O and Al−N bond lengths are in the range of 1.796–1.879 Å and 1.929–1.931 Å, respectively. In configuration **V2**, both O atoms of the N2 nitro group also completely dissociated, and three Al−N bonds and seven Al−O bonds formed (r (Al−O)=1.781–1.919 Å, r (Al−N)=1.940–2.055 Å). The product of **V3** is similar to **V1**, which forms one more Al−N bond of N2 atom (r (Al−N)=2.048 Å). The **V4** configuration decomposed as Formula (2). The adsorptions lead to dissociation of one of nitro O atoms. Both the dissociated and undissociated O atoms interact strongly with neighboring Al atoms to form four Al−O bonds in lengths of 1.844–1.891 Å. Besides the vertical adsorption configurations **V1** to **V4**, we also studied the cases in which the RDX molecule was initially parallel and tilted to the Al surface, as **P1** and **T1**, respectively. In **P1**, our study indicated that the RDX molecule rotates to maximize the interaction with the Al surface during the optimization. As a result, the RDX molecule is nondissociative as shown in Formula (1). The configuration **P1** illustrates that the RDX molecule symmetrically adsorbed on the Al surface, and each O atom forms an Al−O bond with an Al atom underneath (bond lengths are in range of 1.813–1.819 Å). At the same time, the Al atom below the RDX molecular center interacts with three N atoms to form three Al−N bonds (bond lengths are in the range of 2.087–2.095 Å), and in **T1** configuration, the RDX decomposed as Formula (4). The adsorptions lead to the breaking of N−NO_2 bond. The decomposed NO_2 group and the remaining RDX fragment interact strongly with neighboring Al atoms to form two Al−O bonds in lengths of 1.791–1.805 Å and two Al−N bonds in lengths of 1.834–1.933 Å.

As can be seen from Table 1 and Fig. 2, the E_{ads} value of **T1** (−293.1 kJ mol^{-1}) is the smallest, since N−NO_2 bond is a very weak bond, one NO_2 group dissociated from RDX and formed two Al−O bonds and two Al−N bonds. The E_{ads} value of **V4** (−351.5 kJ mol^{-1}) is the second smallest, since there is only one O atom

Table 1 Adsorption energies (E_{ads}), activation energies (E_a) and adsorption sites of RDX on the Al(111) surface

Relation of N1−N2 of RDX molecule with the Al slab	Configurations	Adsorption sites	E_{ads} (kJ mol^{-1})	E_a (kJ mol^{-1})
Vertical	**V1**	top	−798.5	202.9
	V2	hcp	−835.7	143.1
	V3	bridge	−809.2	70.5
	V4	fcc	−351.5	353.1
Parallel	**P1**	spread	−537.4	–
Tilted	**T1**	top [a]	−293.1	121.5

[a]N1 atom on the top site on Al(111) surface.

dissociated and formed four Al−O bonds without any Al −N bond. Otherwise, when two nitro O atoms of RDX molecule are dissociated, the corresponding adsorption energies are very large. The adsorption energy of **V1**, **V2** and **V3** are −798.5, −835.7 and −809.2 kJ mol^{-1}, respectively. Although the decomposition products of **V1**, **V2** and **V3** are similar, the corresponding adsorption energies are different, because there is an additional Al−N bond in **V3** as compared to **V1** (E_{ads} is almost 10.7 kJ mol^{-1} larger), as well as there is an additional Al−O bond in **V2** as compared to **V3** (E_{ads} is almost 26.5 kJ mol^{-1} larger). Although the configuration **P1** forms six Al−O bonds and three Al−N bonds **V3**, the corresponding adsorption energies are much smaller than those of **V3** (almost 271.8 kJ mol^{-1} smaller), because the RDX molecule in **P1** does not dissociate, and there is no bond broken. During the adsorption process, the nitro N and O atoms interact with Al atoms to form weak bonds, and release less energy as compared to **V3**.

As a whole, when the decomposition products of the RDX molecule in **V1**, **V2** and **V3** configurations are of three radical species, their adsorption energies are much larger than those of two radical species and nondissociative configurations. Herein, these radical species readily oxidize the Al and form strong Al−O and Al−N bonds. In a word, for all the above mentioned configurations of RDX except **P1**, the RDX molecule is decomposed to different products when initially being placed on different surface sites, resulting in strong chemical adsorptions. In addition to the formation of strong Al−O bonds, the Al−N bonds are also formed through the strong interaction of nitro N atoms with the surface Al atoms. The fact that the dissociation of the nitro group on the Al(111) surface was observed in simple energy minimizations suggests that the uncoated Al surface is very active to the electron acceptors as further discussed below.

The density of state (DOS)

The electronic structure is intimately related to their fundamental physical and chemical properties. Moreover, the electronic structures and properties are related to the adsorptions and decompositions for the adsorbates. The discussion above suggests that the decomposition of the RDX molecule on the Al surface initiates from the rupture of N−O bond and results in the formation of Al−O and Al−N bonds. Therefore, the knowledge of their electronical properties appears to be useful for further understanding the behaviors of the RDX molecule on the Al surface. Figure 3 displays the total DOS and their projection on the N, O and Al atoms for all adsorption configurations. Clearly, the total DOS equals the sum of its projections on N, O and Al atoms. The electronic structures vary with adsorption configurations due to the differently dissociated products of the RDX molecule.

As can be seen from Fig. 3, for N and O atoms of **P1**, the DOS peak changes greatly, compared to **c**, the peaks disappeared at the energy of 0 eV. The values of the peaks become smaller, while the number of the peaks increases, and the DOS of Al atoms is almost unchanged, as compared to **c**. For **T1** configuration, the peaks also disappeared at the energy of 0 eV for N atoms, and the values of the peaks become smaller, while almost all the peaks split into double ones. For **V1** to **V4** configurations, the DOS of O atoms are similar to each others in **V1**, **V3** and **V4** configurations. Their highest

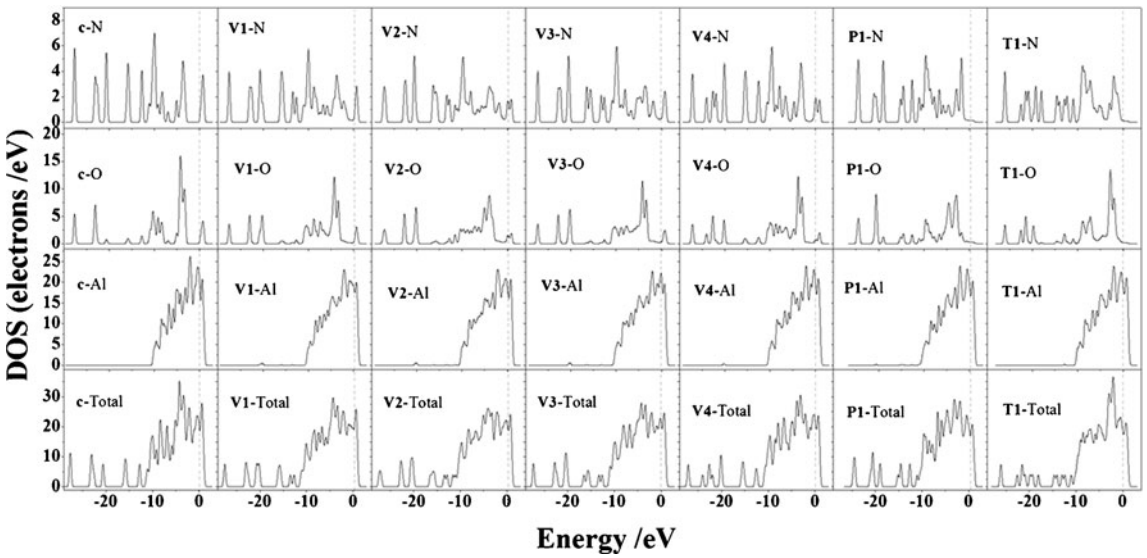

Fig. 3 Total DOS and their projections on the N, O, and Al atoms for all adsorption configurations. **c** is a non-adsorption configuration

peaks of DOS for O atoms become smaller than those of **c** at the energy of −5 eV, and the peaks become smoother, whereas the number of DOS peaks becomes more in the range of −10 to −5 eV, as compared to **c**. For **V2**, the peak of the DOS projection on O atoms becomes smaller because of one more Al−O bond formed. The peaks of DOS become smoother in the range of −10 to 0 eV, as compared to **V1**, **V3** and **V4** configurations. At the same time, the DOS on N atom of **V1**, **V2** and **V3** are similar, the peaks become lower and smoother in the range of −10 to 0 eV. It is because that there are two to three Al−N bonds formed in these three configurations. And for **V4**, because there is no Al−N bond formed, the DOS of N atoms almost does not change between −10 and 0 eV. From the above analysis we can draw that when bonding interactions between the absorbates and the Al surface are strengthened, the DOS shifts and becomes smoother with respect to those of **c**. These explain the dissociation of N−O bonds and the formation of strong Al−O and Al−N bonds. In addition, the lower the DOS peak number of N and O atoms, the greater the number of the formation of Al−O and Al−N bonds.

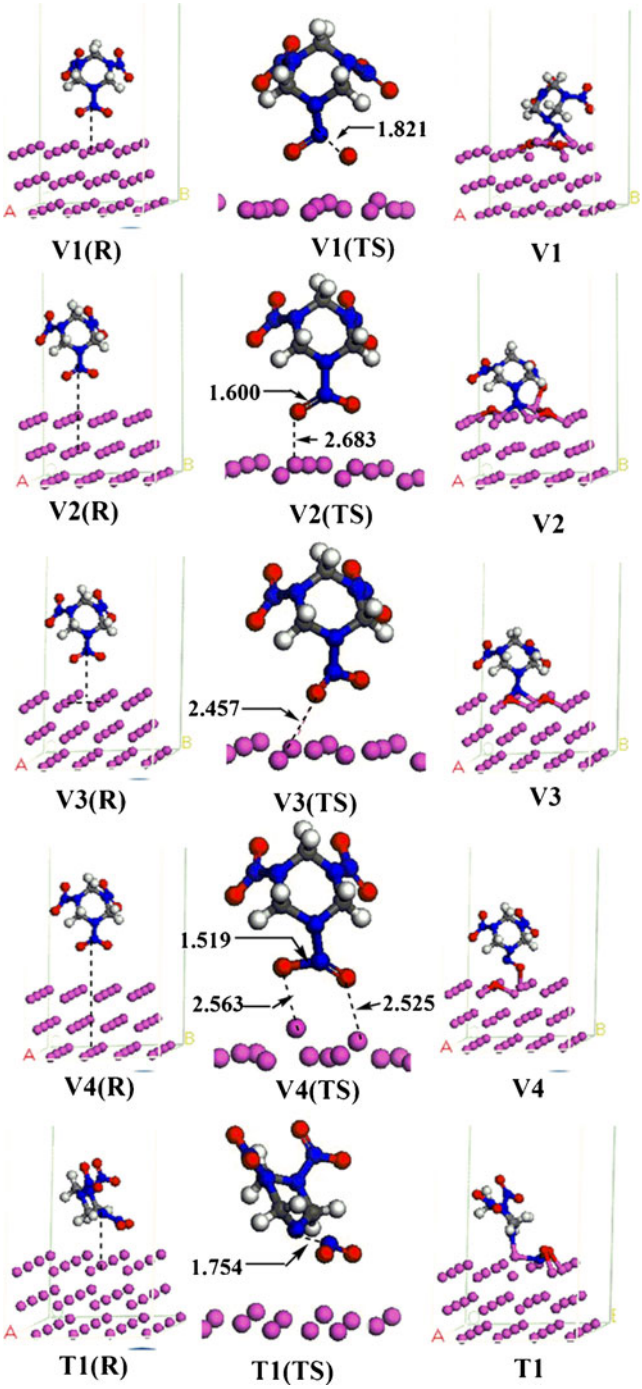

Fig. 4 Lateral views of RDX on the Al(111) surface. The index **R** and **TS** denote the reactant and transition state, respectively

The mechanism of dissociation

The reactants (R), transition state (TS) and products for the surface reaction of RDX molecule on the Al(111) were depicted in Fig. 4, and a detailed energy profile for four dissociation of adsorbed RDX configurations were presented in Fig. 5. The activation energies and reaction energies at transition state were tabulated in Table 1. As can be seen from Fig. 4, the RDX molecule interacts with several Al atoms that deviate from the Al surface obviously for **V1(TS)**. The O2 atom moves away from N2 atom, as the distance between N2 and O2 increases from 1.218 to 1.821 Å, while the distance between N2 and O1 increases from 1.225 to 1.415 Å. The activation energy (E_a) of this transition state is 202.9 kJ mol^{-1} (see Table 1 and Fig. 5), indicating that this process is hard to occur. In the decomposition process, the O2 atom keeps moving to the Al surface, and the O1 atom also leaves the N2 atom. These two O atoms bind with the surface Al atoms and form six Al−O bonds. In addition, another two Al−N bonds (between N2 atom and two surface Al atoms) come into being. For **V2(TS)** and **V3(TS)**, the RDX

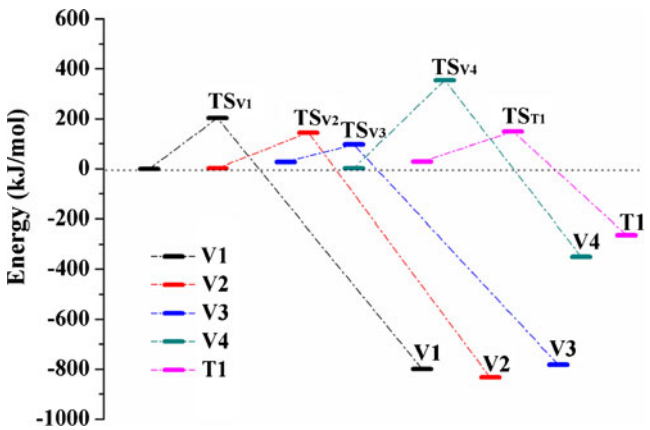

Fig. 5 Relative energy profile for RDX decomposition on the Al(111) surfaces

molecule does not decompose in these two states, as compared to the local minimum of physical adsorptions, the RDX molecule moves down toward the Al surface and interacts with surface Al atoms. As a result, some Al atoms deviate from the Al surface obviously. Compared to the initial state, the bond length of N2−O1 bond in **V2(TS)** increases from 1.252 to 1.600 Å and those in **V3(TS)** increases from 1.252 to 1.314 Å, while the bond angle θ(O1−N2−O2) in **V2(TS)** decreases from 126.8° to 114.9° and in **V3(TS)** decreases from 126.8° to 121.9°. With the reaction going on, two O atoms dissociated from N2 atom. The distances between the partially dissociated O1 atoms and the nearest Al atoms decrease from 3.639 to 2.683 Å (**V2**) and from 3.736 to 2.457 Å (**V3**). The activation energies (E_a) are 143.1 and 70.5 kJ mol^{-1}, respectively (Table 1 and Fig. 5). After the transition state, the N2−O1 and N2−O2 bonds rupture. The dissociated moiety binds to the surface and forms seven Al−O and three Al−N bonds (in **V2**) and six Al−O and two Al−N bonds (in **V3**).

Then for **V4(TS)**, compared to the local minimum of physical adsorption, the RDX molecule moves toward the Al surface and attracts two Al atoms that deviate from the Al surface obviously, and the bond length of N2−O1 bond increases from 1.252 to 1.519 Å, while the distances between the O1 and O2 atoms and the nearest Al atoms both decrease from 2.916 to 2.563 Å and 3.025 to 2.525 Å, respectively. The activation barrier (E_a) of **V4(TS)** is 353.1 kJ mol^{-1} (see Table 1 and Fig. 5), which means that this process is hard to occur. With the reaction going on, the O1 atoms dissociated from N2 atom, and O1 atom move apart from N2 atom and the dissociated moiety binds to the surface and forms four Al−O interactions (see **V4**).

Finally, for **T1 (TS)**, the RDX molecule interacts with Al surface where one Al atom obviously deviates from the Al surface. The NO_2 group moves away from RDX, as the distance between N1 and N2 increases from 1.402 to 1.754 Å. The activation energy (E_a) of this transition state is 121.5 kJ mol^{-1} (see Table 1 and Fig. 5). With the decomposition process going on, the NO_2 group departures away from the remaining moiety of RDX. At the meantime, both the NO_2 and the remaining fragment of RDX move toward the Al surface. These two fragments bind with the surface Al atoms and form two Al−O bonds and two Al−N bonds (see **T1**). Although the N−NO_2 bond is the weakest bond in isolated RDX, the N−O is even easier to decompose on the Al(111) surface.

Conclusions

Based on the investigation of RDX molecule on Al(111) surface, the major findings can be summarized as follows.

(1) There exist chemical adsorptions when the RDX molecule approaches the Al surface. The Al surface is readily oxidized by the oxygen-rich nitro group of the dissociatively adsorbed RDX. Dissociations of the N−NO_2 bond and N−O bonds of nitro group result in the formations of strong Al−O and Al−N bonds. As the number of the formations of Al−O and Al−N bonds increases, the corresponding adsorption energy increases greatly.

(2) The DOS projections on the N and O atoms for the dissociated N−O bonds and N−NO_2 bond adsorptions occur with an obvious shift of peaks, which infers that energy bands become broad and the interactions of chemical bonds are strengthened.

(3) The decomposition processes on Al surface are predicted to be exothermic. The activation energy for **V4** configuration is as large as 353.1 kJ mol^{-1}. However, the activation energies of other configurations are in the range of 53.7 to 202.9 kJ mol^{-1}.

(4) Although the N−NO_2 bond is the weakest bond in isolated RDX, the N−O is even easier to decompose on the Al(111) surface.

Acknowledgments We gratefully acknowledge the funding provided by the Laboratory of Science and Technology on Combustion and Explosion (Grant No. 9140C3501021101) for supporting this work. Cai-Chao Ye thanks the Innovation Foundation from the Graduate School of Nanjing University of Science and Technology for partial financial support.

References

1. Sutton GP (1992) Rocket propulsion elements. Wiley, New York
2. Wang RH, Guo Y, Sa R, Shreeve JM (2010) Chem Eur J 16:8522–8529
3. Singh RP, Shreeve JM (2011) Chem Eur J 17:11876–11881
4. Chakraborty D, Muller RP, Dasgupta S, Goddard WA (2000) J Phys Chem A 104:2261–2272
5. Boyd S, Murray JS, Politzer P (2009) J Chem Phys 131:204903
6. Umezawa N, Kalia RK, Nakano A, Vashista P, Shimojo F (2007) J Chem Phys 126:234702
7. Millar DIA, Oswald IDH, Francis DJ, Marshall WG, Pulham CR, Cumming AS (2009) Chem Commun:562–564
8. Hakey P, Ouellette W, Zubieta J, Korter T (2008) Acta Crystallogr Sect E 64:o1428
9. Ciezak JA, Jenkins TA (2008) Propell Explos Pyrot 33:390–395
10. Zhang JG, Wang K, Niu XQ, Zhang SW, Feng XJ, Zhang TL, Zhou ZN (2012) J Mol Model 18:3915–3926
11. Scott AM, Petrova T, Odbadrakh K, Nicholson DM, Fuentes-Cabrera M, Lewis JP, Hill FC, Leszczynski J (2012) J Mol Model 18:3363–3378
12. Guadarrama-Perez C, de La Hoz JMM, Balbuena PB (2010) J Phys Chem A 114:2284–2292
13. Price EW (1984) Fundamentals of solid-propellant combustion. Progress in astronautics and aeronautics. American Institute of Aeronautics and Astronautics, New York
14. Zhu J, Li SF (1999) Propell Explos Pyrot 24:224–226
15. Zhou SQ, Zhao FQ, Ju XH, Cheng XC, Yi JH (2010) J Phys Chem C 114:9390–9397

16. Thompson DL, Sorescu DC, Boatz JA (2005) J Phys Chem B 109:1451–1463
17. Sorescu DC, Boatz JA, Thompson DL (2003) J Phys Chem B 107:8953–8964
18. Sorescu DC, Boatz JA, Thompson DL (2004) Proceedings Users Group Conference, pp 2–6
19. Ye CC, Ju XH, Zhao FQ, Xu SY (2012) Chin J Chem 30:2539–2548
20. Johnson O (1973) J Catal 28:503–505
21. Hoffmann R (1988) Solids and surfaces: A chemist's view of bonding in the extended structures. VCH, New York
22. Chatterjee A, Niwa S, Mizukami F (2005) J Mol Graph 23:447–456
23. Tian K, Tu XY, Dai SS (2007) Surf Sci 601:3186–3195
24. Alfonso DR (2008) Surf Sci 602:2758–2768
25. Alfonso DR, Cugini AV, Sorescu DC (2005) Catal Today 99:315–322
26. Segall MD, Lindan PJD, Probert MJ, Pickard CJ, Hasnip PJ, Clark SJ, Payne MC (2002) J Phys Condens Mat 14:2717–2744
27. Perdew JP, Jackson KA, Pederson MR, Singh DJ, Fiolhais C (1992) Phys Rev B 46:6671–6687
28. Perdew JP, Burke K, Ernzerhof M (1996) Phys Rev Lett 77:3865–3868
29. Kresse G (1996) Phys Rev B 54:11169–11186
30. Fischer TH, Almlof J (1992) J Phys Chem 96:9768–9774
31. King HW (2000) CRC handbook of chemistry and physics, 81st edn. CRC, Boca Raton
32. Halgren TA, Lipscomb WN (1977) Chem Phys Lett 49:225–232